



Optics Letters

Experimental mitigation of the effects of the limited size aperture or misalignment by singular-value-decomposition-based beam orthogonalization in a free-space optical link using Laguerre–Gaussian modes

KAI PANG,^{1,*} HAOQIAN SONG,¹ XINZHOU SU,¹ KAIHENG ZOU,¹ ZHE ZHAO,¹ HAO SONG,¹ AHMED ALMAIMAN,^{1,2} RUNZHOU ZHANG,¹ CONG LIU,¹ NANZHE HU,¹ SHLOMO ZACH,³ NADAV COHEN,³ BRITTANY LYNN,⁴ ANDREAS F. MOLISCH,¹ ROBERT W. BOYD,⁵ MOSHE TUR,³ AND ALAN E. WILLNER¹

¹Department of Electrical Engineering, University of Southern California, Los Angeles, California 90089, USA

²King Saud University, Riyadh 11362, Saudi Arabia

³School of Electrical Engineering, Tel Aviv University, Ramat Aviv 69978, Israel

⁴Naval Information Warfare Center, Pacific, San Diego, California 92152, USA

⁵The Institute of Optics, University of Rochester, Rochester, New York 14627, USA

*Corresponding author: kaipang@usc.edu

Received 14 August 2020; revised 8 October 2020; accepted 12 October 2020; posted 12 October 2020 (Doc. ID 405399); published 13 November 2020

Limited-size receiver (Rx) apertures and transmitter–Rx (Tx–Rx) misalignments could induce power loss and modal crosstalk in a mode-multiplexed free-space link. We experimentally demonstrate the mitigation of these impairments in a 400 Gbit/s four-data-channel free-space optical link. To mitigate the above degradations, our approach of singular-value-decomposition-based (SVD-based) beam orthogonalization includes (1) measuring the transmission matrix H for the link given a limited-size aperture or misalignment; (2) performing SVD on the transmission matrix to find the U , Σ , and V complex matrices; (3) transmitting each data channel on a beam that is a combination of Laguerre–Gaussian modes with complex weights according to the V matrix; and (4) applying the U matrix to the channel demultiplexer at the Rx. Compared with the case of transmitting each channel on a beam using a single mode, our experimental results when transmitting multi-mode beams show that (a) with a limited-size aperture, the power loss and crosstalk could be reduced by ~ 8 and ~ 23 dB, respectively; and (b) with misalignment, the power loss and crosstalk could be reduced by ~ 15 and ~ 40 dB, respectively. © 2020 Optical Society of America

<https://doi.org/10.1364/OL.405399>

Space-division-multiplexing (SDM) has the potential to further increase the total capacity of a free-space optical (FSO) link, since multiple independent data-carrying beams can be simultaneously transmitted [1]. One subset of SDM is mode-division-multiplexing (MDM), in which each data-carrying

beam occupies a different orthogonal spatial mode from a modal basis set [2,3]. With MDM, little inherent crosstalk is induced when multiplexing at the transmitter (Tx) aperture, spatially co-propagating, and demultiplexing at the receiver (Rx) aperture [4].

One example of an orthogonal modal set is Laguerre–Gaussian (LG) beams that form a two-dimensional $\{l, p\}$ set in which (1) l represents the number of 2π phase shifts in the azimuthal direction of the phase front, and (2) $p + 1$ represents the number of radial intensity nodes (e.g., rings) [5]. An MDM link can multiplex multiple beams, each composed of a single LG mode [4,6–8]. Unfortunately, such MDM FSO links can be affected by a limited-size Rx aperture or misalignments between the Tx and Rx apertures. These two issues can cause deleterious signal-power loss and modal-power-coupling crosstalk in MDM links in which each channel is transmitted on a beam using a single LG mode [9–14].

In general, approaches that were utilized to reduce the modal crosstalk caused by a limited-aperture Rx include the following: (1) each data channel is transmitted on a beam composed of one carefully selected orbital angular momentum mode such that the received channels on different beams remain orthogonal [12,13]; and (2) specific modes at the Tx and an Rx aperture are carefully chosen to reduce the crosstalk such that cross-coupling does not significantly appear at the other channel [14].

In our approach, each data channel is transmitted on a single beam composed of a unique set of LG modes. By carefully designing the modal complex weights, all data channels could be spatially tailored and remain orthogonal at the Rx. This could

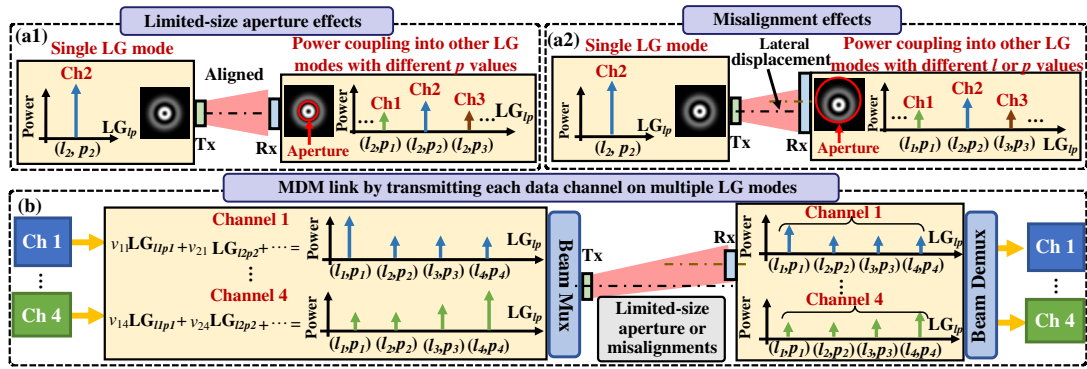


Fig. 1. (a) Concept of (a1) a limited-size aperture and (a2) misalignment effects on an FSO link using LG modes. (b) Concept diagram of transmitting each data channel on a designed beam that is a combination of multiple LG modes (multi-mode beam) to mitigate the effects of the limited-size aperture or misalignments in an MDM link. Ch, channel; Tx, transmitter; Rx, receiver.

simultaneously mitigate power loss and crosstalk induced by limited-size apertures or misalignments.

In this Letter, we experimentally demonstrate the utilization of our approach in a 400 Gbit/s four-channel FSO link. We follow these steps: (1) measure the transmission matrix \mathbf{H} for the link that has a limited-size aperture or misalignments, (2) perform SVD \mathbf{H} to find the \mathbf{U} , $\mathbf{\Sigma}$, and \mathbf{V} complex matrices, (3) transmit each data channel on multi-mode beam with weights according to the \mathbf{V} matrix, and (4) apply the \mathbf{U} matrix to the Rx demultiplexer. The experimental results when transmitting multi-mode beams show that (a) with a limited-size aperture, the power loss and crosstalk could be reduced by ~ 8 and ~ 23 dB, respectively; and (b) with misalignments, the power loss and crosstalk could be reduced by ~ 15 and ~ 40 dB, respectively.

In a LG mode-multiplexed FSO link, if the Rx aperture is limited, only a part of the power would be collected. Moreover, this issue could also cause power coupling to other LG modes with the same l value but different p values, thereby increasing both power loss and crosstalk, as shown in Fig. 1(a1) [10]. In addition, when there is a Tx–Rx misalignment, the power on the desired LG mode would be coupled to other LG modes with different l or p values. This could induce both power loss and crosstalk, as shown in Fig. 1(a2) [9].

Figure 1(b) presents the concept of transmitting each data channel on a multi-mode beam to mitigate the effects of the limited-size aperture or misalignments in an MDM link. Generally, the mode coupling between a set of LG modes in a given link can be described as \mathbf{H} [8]. Our approach is based on SVD of \mathbf{H} ($\mathbf{H} = \mathbf{U} \cdot \mathbf{\Sigma} \cdot \mathbf{V}^*$), which is usually utilized to find orthogonal basis at the Tx and Rx with no interference between data channels [15–17]. At the Tx, the multi-mode beams are generated by complex combinations of multiple LG modes, of which the complex weights are given by the orthogonal column vectors of the \mathbf{V} . After passing through a given link with a limited-size aperture or misalignments, the resulting beams on different channels are still composed of multiple LG modes, of which the complex weights are the orthogonal row vectors multiplied by the singular values in the $\mathbf{\Sigma}$ matrix. This means that these beams are still orthogonal and thus can be demultiplexed with little crosstalk based on the orthogonal row vectors of the inverse of the \mathbf{U} matrix. Besides, the intensity profiles of

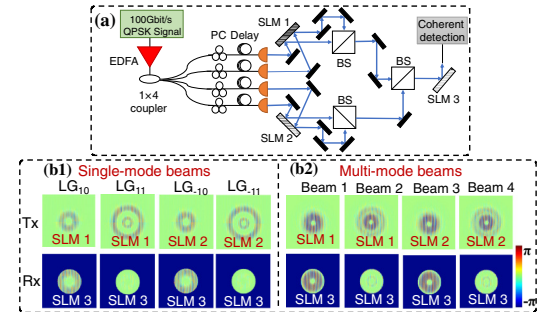


Fig. 2. (a) Experimental setup of a four-channel MDM FSO system. QPSK, quadrature phase-shift keying; EDFA, erbium-doped fiber amplifier; PC, polarization controller; Col., collimator; SLM, spatial light modulator; BS, beam splitter. (b) Tx and Rx SLM patterns for (b1) single-mode beams and (b2) designed multi-mode beams. Here the radius of an Rx aperture is 1.0 mm.

the transmitted beams would be spatially shaped, which might also reduce the power loss.

Figure 2 shows the experimental setup of a four-channel MDM FSO link. At the Tx, a 100 Gbit/s quadrature phase-shift keying (QPSK) signal at 1550 nm is amplified by an erbium-doped fiber amplifier (EDFA) and subsequently equally split into four branches by a 1×4 coupler. All the four copies are delayed by single-mode fibers with different lengths to decorrelate the data sequences. Subsequently, each branch is sent into a collimator that generates a collimated Gaussian beam with a diameter of 3 mm. The Gaussian beams are sent to two spatial light modulators (SLMs) loaded with different phase holograms on each half of the screen to create specific beams. These four outputs are multiplexed and coaxially propagate in free space over ~ 1 m. At the Rx, SLM 3 is loaded with a specific phase pattern to convert one of the incoming beams to a Gaussian-like beam. Finally, it is coupled to an SMF for coherent detection and bit error rate (BER) measurements.

Our method includes the following steps. (1) Measure \mathbf{H} for a set of LG modes using the method in [8]. (2) Calculate the SVD of \mathbf{H} by $\mathbf{H} = \mathbf{U} \cdot \mathbf{\Sigma} \cdot \mathbf{V}^*$. (3) At the Tx, utilize different columns of matrix \mathbf{V} to design mutually orthogonal multi-mode beams, each of which is a complex combination of multiple LG modes

and carries one of the four data channels. Subsequently, we construct the phase patterns on the SLM (1 and 2) for orthogonal multi-mode beams using the approach in [8]. (4) At the Rx, utilize different rows of the inverse matrix \mathbf{U} to construct the phase patterns on SLM 3 that can convert the incoming multi-mode beam back to a Gaussian-like beam [8]. As an example, when the radius of the Rx aperture is 1.0 mm, the Tx and Rx SLM patterns for single-mode beams and multi-mode beams are shown in Figs. 2(b1) and 2(b2), respectively. We note that, since the generation of orthogonal beams depends on the exact channel matrix, the Tx and Rx SLM patterns should be different under different aperture sizes or misalignments in our approach.

First, we evaluate the effect of the Rx aperture size on the MDM link when transmitting data channels 1 and 2 (Ch 1 and 2) on a single LG_{10} and LG_{11} mode, respectively, as shown in Fig. 3(a1). It should be noted that the “Ch 1” and “Ch 2” in the following figures carry the same meaning as the ones in Fig. 2. At the Tx, we generate a single LG_{10} or LG_{11} beam with a beam radius of 0.7 mm by using the SLM. After propagating through the free space, LG_{10} and LG_{11} beams have beam sizes of ~ 1.3 and ~ 1.8 mm at the Rx, respectively. The phase patterns on SLM-3 have circular aperture shapes, whose radii are defined as aperture sizes in our experiment. As expected, the power loss increases as the aperture size decreases, as shown in Fig. 3(b1). In addition, we measured channel crosstalk that refers to the power coupled from the other modes over the power on the desired mode. We see that the crosstalk for both LG beams becomes higher when decreasing the aperture size. This is because a limited-size aperture blocks a part of the LG beams, thus degrading the orthogonality between LG modes with different p values [10]. In our approach, the data channel is transmitted on a multi-mode beam. Since the limited-size aperture affects the beam profiles in the radial direction, multiple LG modes with different p values are utilized to tailor the profiles of multi-mode beams in the radial direction, as shown in Fig. 3(a1). However, we find that there would be a relatively high power loss if we only use the same two LG modes (LG_{10} , and LG_{11}) as the case of single-mode beams. Therefore, an extra LG mode (LG_{12}) is utilized in the generation of multi-mode beams. Theoretically, the power loss of the multi-mode beams is related to the diagonal elements in the \sum matrix [15]. We see that power loss for both channels is reduced with an aperture radius of 1.0–1.6 mm. In addition, we find that when the aperture radius is less than 0.8 mm, the power loss of the multi-mode beam-carrying data channel 2 would become even larger. This might be due to the variation of \mathbf{H} with the aperture radius. As the aperture radius decreases, the power coupling from the desired single LG mode to the other LG modes gradually increases and becomes similar to the power on the desired LG mode [10]. This results in a smaller difference between the values of diagonal elements and off-diagonal elements in \mathbf{H} . Consequently, this would induce a decrease in the value of the second diagonal element in the \sum matrix after SVD calculation of \mathbf{H} , which causes an increase in the power loss for the second multi-mode beam.

Moreover, the crosstalk between the two channels is also reduced, which is because the orthogonality between the two beams is not degraded by the limited-size aperture. We also note that the crosstalk for channel 2 increases when the aperture radius is less than 0.8 mm. This is mainly due to a large power loss of the multi-mode beam-carrying channel 2 under a small aperture size, which will cause a higher crosstalk that refers to the ratio of power coupled from the other multi-mode beam

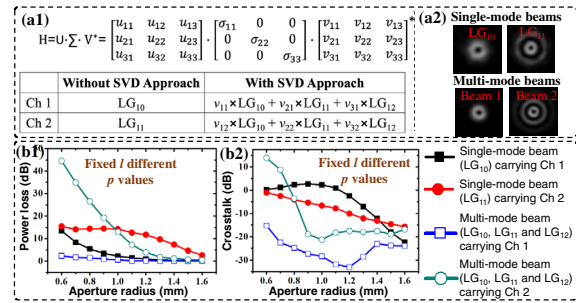


Fig. 3. (a1) Complex weights of LG mode-carrying data channels 1 and 2 without and with the SVD approach; (a2) measured intensity profiles of single-mode beams and multi-mode beams when the aperture radius is 1.0 mm. (b) Measured limited-size-aperture induced (b1) power loss and (b2) crosstalk under various aperture radii when transmitting data channels on single-mode beams or multi-mode beams. For each aperture radius, the two multi-mode beams are unique due to different transmission matrices.

to the power of the desired multi-mode beam. Moreover, it could be expected that when using additional LG modes with higher p values, the performance of these two channels might be further improved. This might be due to more sophisticated control of the multi-mode beam’s spatial profile in the radial direction by using additional LG modes with higher p values [18]. As an example, the experimental intensity profiles of single-mode beams and multi-mode beams with an aperture radius of 1.0 mm are shown in Fig. 3(a2). The intensity profiles of multi-mode beams vary with the aperture radius according to the SVD calculations of transmission matrices for different aperture radii. This results in different power losses with the aperture radius, as shown in Fig. 3(b1). We can see that when the aperture radius is 1.0 mm, both multi-mode beams are smaller than single-mode beams, which results in lower power losses.

The influence of horizontal displacements on system performance is also investigated. As shown in Fig. 4(a), when transmitting data channels on single-mode beams with different p values (LG_{10} , LG_{11}), both the power loss and crosstalk become larger with horizontal displacements. In our approach, the same two LG modes (LG_{10} , LG_{11}) are utilized to generate the multi-mode beams. Compared with the case of single-mode beams, the power loss for both channels is reduced within a displacement range of 0.4–0.7 mm. In addition, the crosstalk for both multi-mode beams remains at a relatively low level (< -27 dB) with the displacement. Furthermore, we also explore the effects of displacements on LG modes with different l values (LG_{10} , LG_{-10}), as shown in Fig. 4(b). It is observed that the power loss and crosstalk of LG_{10} , LG_{-10} modes increase with the displacement. For both channels, the power loss can be reduced when using the multi-mode beams (composed of LG_{10} , LG_{-10} modes) with a displacement range of 0.8–1.1 mm. Moreover, the crosstalk for both channels stays at a relatively low level (< -17 dB) with the displacement. We also find an increase and then a decrease of the power loss for the second beam with the displacement in Fig. 4. This might be due to the change of \mathbf{H} with the displacement [13]. First, the power coupling from the desired single LG mode to the other LG mode gradually increases and becomes similar to the power of the desired LG mode with the displacement. This results in a smaller difference between the values of diagonal elements and off-diagonal elements in \mathbf{H} . Consequently, this would induce a

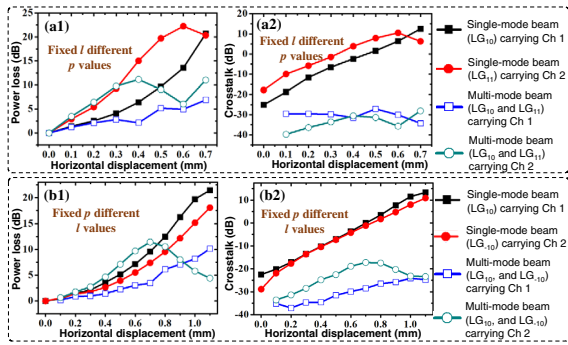


Fig. 4. (a) Measured displacement-induced (a1), (b1) power loss and (a2), (b2) channel crosstalk with horizontal displacements when transmitting channels on single-mode beams or multi-mode beams.

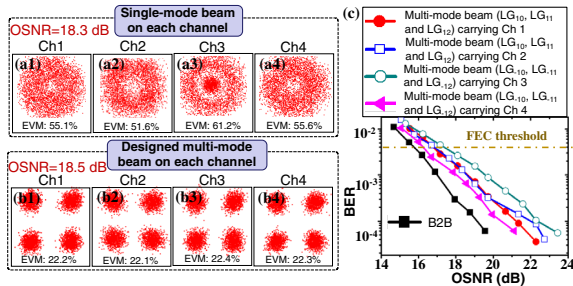


Fig. 5. Measured constellations when transmitting each channel on (a) a single-mode beam or (b) a multi-mode beam. (c) Experimental BERs of four data channels with an optical signal-to-noise ratio (OSNR) when transmitting each channel on one of the multi-mode beams. B2B, back to back; FEC, forward error correction.

decrease in the value of the second diagonal element in the Σ matrix, which causes an increase in the power loss for the second beam. However, as the power coupling continually increases with the displacement, it would be higher than the power in the desired LG mode. Therefore, the difference between the values of diagonal elements and other elements in H will increase. As a result, the value of the second diagonal element in the Σ matrix would increase, which causes the power loss of the multi-mode beam to decrease [15].

We subsequently utilize our approach in a four-channel multiplexed link, each carrying a 100 Gbit/s QPSK signal as shown in Fig. 5. Specifically, four single-mode-beams (LG_{10} , LG_{11} , LG_{-10} , and LG_{-11}) or four multi-mode beams are utilized. Here the aperture radius is 1.0 mm, and there is no displacement. In the case of single-mode beams, all four channels have high error vector magnitude (EVM) ($> 50\%$). This is due to their higher crosstalk caused by the limited-size aperture. However, when using the multi-mode beams, the EVM of the four channels are all relatively low ($\sim 22\%$). First, two multi-mode beams are composed of LG_{10} , LG_{11} , and LG_{12} modes, while other two multi-mode beams are composed of LG_{-10} , LG_{-11} , and LG_{-12} modes. In BER measurements, the power penalties of all four channels are < 2 dB at the 7%-overhead forward error correction (FEC) limit.

In this Letter, we utilized the SVD-based beam orthogonalization to mitigate the effects of the limited-size aperture or misalignments. Moreover, we note that the beam size and

direction can be further tailored by adding transfer functions of a lens and a linear grating on the Tx-side SLM, respectively [19,20]. Therefore, this might be an effective complement to our approach and further improve the system performance. Furthermore, we note that it might also be possible to utilize the SVD-based beam orthogonalization to mitigate other issues in an MDM FSO link, such as atmospheric turbulence [8].

Funding. National Science Foundation (ECCS-1509965); Vannevar Bush Faculty Fellowship sponsored by the Basic Research Office of the Assistant Secretary of Defense (ASD) for Research and Engineering (RE) and funded by the Office of Naval Research (ONR) (N00014-16-1-2813); Defense Security Cooperation Agency (DSCA-4440646262); Office of Naval Research through a MURI grant (N00014-20-1-2558); Airbus Institute for Engineering Research.

Disclosures. The authors declare no conflicts of interest.

REFERENCES

- D. J. Richardson, J. M. Fini, and L. E. Nelson, *Nat. Photonics* **7**, 354 (2013).
- G. Gibson, J. Courtial, M. J. Padgett, M. Vasnetsov, V. Pasko, S. M. Barnett, and S. Franke-Arnold, *Opt. Express* **12**, 5448 (2004).
- I. B. Djordjevic, *Opt. Express* **19**, 14277 (2011).
- K. Pang, H. Song, Z. Zhao, R. Zhang, H. Song, G. Xie, L. Li, C. Liu, J. Du, A. F. Molisch, M. Tur, and A. E. Willner, *Opt. Lett.* **43**, 3889 (2018).
- R. L. Phillips and L. C. Andrews, *Appl. Opt.* **22**, 643 (1983).
- J. Wang, J.-Y. Yang, I. Fazal, N. Ahmed, Y. Yan, H. Huang, Y. Ren, Y. Yue, S. Dolinar, M. Tur, and A. E. Willner, *Nat. Photonics* **6**, 488 (2012).
- L. Allen, M. W. Beijersbergen, R. J. C. Spreeuw, and J. P. Woerdman, *Phys. Rev. A* **45**, 8185 (1992).
- H. Song, H. Song, R. Zhang, K. Manukyan, L. Li, Z. Zhao, C. Liu, A. Almaiman, R. Bock, B. Lynn, M. Tur, and A. E. Willner, *J. Lightwave Technol.* **38**, 82 (2020).
- G. Xie, L. Li, Y. Ren, H. Huang, Y. Yan, N. Ahmed, Z. Zhao, M. P. J. Lavery, N. Ashrafi, S. Ashrafi, R. Bock, M. Tur, A. F. Molisch, and A. E. Willner, *Optica* **2**, 357 (2015).
- X. Zhong, Y. Zhao, G. Ren, S. He, and Z. Wu, *IEEE Access* **6**, 8742 (2018).
- K. Pang, H. Song, X. Su, K. Zou, Z. Zhao, H. Song, A. Almaiman, R. Zhang, C. Liu, N. Hu, S. Zach, N. Cohen, B. Lynn, A. F. Molisch, R. W. Boyd, M. Tur, and A. E. Willner, in *Optical Fiber Communications Conference* (Optical Society of America, 2020), paper W1G. 2.
- S. Zheng, X. Hui, J. Zhu, H. Chi, X. Jin, S. Yu, and X. Zhang, *Opt. Express* **23**, 12251 (2015).
- G. Xie, Y. Xiong, H. Huang, N. Ahmed, L. Li, Y. Yan, M. P. J. Lavery, M. J. Padgett, M. Tur, and S. J. Dolinar, in *Conference on Lasers and Electro-Optics* (2014), paper SM3J.2.
- G. Xie, Y. Xiong, H. Huang, Y. Yan, C. Bao, N. Ahmed, M. Willner, M. P. J. Lavery, M. J. Padgett, and A. E. Willner, in *2013 IEEE Globecom Workshops* (2013), pp. 1116–1120.
- I. E. Telatar, *Eur. Trans. Telecommun.* **10**, 585 (1999).
- G. Lebrun, J. Gao, and M. Faulkner, *IEEE Trans. Wireless Commun.* **4**, 757 (2005).
- W. Liu, L. L. Yang, and L. Hanzo, *IEEE Trans. Veh. Technol.* **58**, 1016 (2008).
- G. Xie, C. Liu, L. Li, Y. Ren, Z. Zhao, Y. Yan, N. Ahmed, Z. Wang, A. J. Willner, C. Bao, Y. Cao, P. Liao, M. Ziyadi, A. Almaiman, S. Ashrafi, M. Tur, and A. E. Willner, *Opt. Lett.* **42**, 991 (2017).
- F. Feng, I. H. White, and T. D. Wilkinson, *J. Lightwave Technol.* **31**, 2001 (2013).
- S. M. Kim and S. M. Kim, *Opt. Eng.* **52**, 106101 (2013).